EASR

Engineering and Applied Science Research

https://www.tci-thaijo.org/index.php/easr/index

Published by the Faculty of Engineering, Khon Kaen University, Thailand

Classifying white blood cells from a peripheral blood smear image using a histogram of oriented gradient feature of nuclei shapes

Anas Mohd Noor*[1)], Haniza Yazid[1)], Zulkarnay Zakaria[1)] and Aishah Mohd Noor[2)]

[1)]School of Mechatronic Engineering, Universiti Malaysia Perlis, 02600 Arau, Perlis, Malaysia
[2)]Institute of Engineering Mathematics, Universiti Malaysia Perlis, 02600 Arau, Perlis, Malaysia

Received 7 August 2019
Revised 23 October 2019
Accepted 8 November 2019

Abstract

Researchers developed various methods and algorithms to classify white blood cells (WBCs) from blood smear images to assist hematologists and to develop an automatic system. Furthermore, the pathological and hematological conditions of WBCs are related to diseases that can be analyzed accurately in a short time. In this work, we proposed a simple technique for WBC classification from a peripheral blood smear image based on the types of cell nuclei. The developed algorithms utilized a histogram of oriented gradient (HOG) feature typically known for application in human disease detection. The segmentation of WBC nuclei utilizes a YCbCr color space and K-means clustering techniques. The HOG feature contains information about the cell nuclei shapes, which then is classified using a support vector machine (SVM) and backpropagation artificial neural network (ANN). The results show that the proposed HOG feature is useful for WBC classification based on the shapes of nuclei. We are able to categorize the type of a WBC based on its nucleus shape with more than 95% accuracy.

Keywords: Histogram of oriented gradient, K-means clustering, YCbCr color space, WBC classification, Microscopic blood smear image

1. Introduction

Microscopic analysis of a peripheral blood film, i.e., a blood smear, provides information on the number and shapes of cells. This information is highly crucial in the early steps in diagnosing hematological disorders or other related medical conditions [1]. For example, the analysis of white blood cells (WBCs) is essential where information such as counts of specific cells (e.g., neutrophils, eosinophils, basophils, lymphocytes, and monocytes) provides information about how a body is responding to a particular medicine or condition. However, the standard laboratory practice requires a manual technique and relies on experts for the blood smear image analysis. This practice is tedious and time-consuming. Machine-based automatic analysis reduces human errors, improves accuracy, and minimizes the required time for analysis. Automatic detection and classification of white blood cells in blood smear images can accelerate the process tremendously [2-4]. An automated cell classification system usually consists of an image acquisition system, image processing such as image segmentation, feature extraction, classification, and interpretation for further evaluation by experts. For instance, the objective of feature extraction is to reveal a set of features from an image of interest, such as textures, lines, corners, and colors. These features must be informative or unique with respect to the desired properties of the original image. Furthermore, the number of features extracted from an image of interest improves the accuracy of image classification. Generally, the classification process includes image segmentation, feature extraction, and interpretation. Currently, various algorithms can be used to classify the input features. However, the accuracy of classification depends only on use of suitable algorithms. Therefore, it is essential to analyze which algorithms are most suitable for a particular application. Typically, the process of WBC classification includes cell detection using machine learning and artificial intelligence algorithms. This has been widely studied to assist human-experts in identifying or providing a pre-classification of characterized blood cells [5-6]. However, WBC classification accuracy is greatly influenced by segmentation and feature extraction processes [7-8]. Therefore, it remains a challenge in image processing and computer vision.

2. Related work

Most of the selected attributes used for classifying the WBCs in a blood smear image are morphological in nature such as geometric [9-10], texture or statistical [11-14], color [15] shape [16-17], and spatial frequency features [18-19].

*Corresponding author.
Email address: anasnoor@unimap.edu.my
doi: 10.14456/easr.2020.13

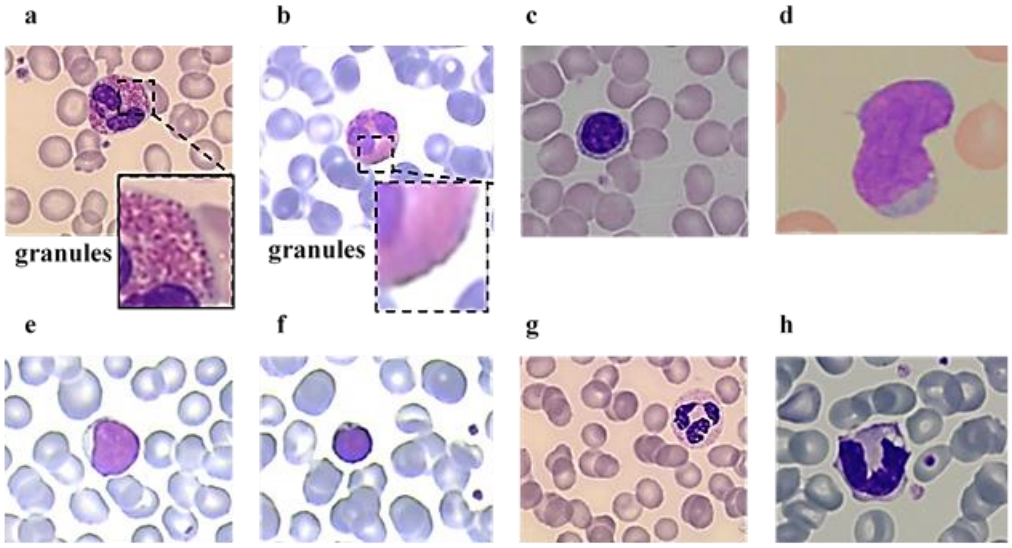

Figure 1 Example of microscopic peripheral blood smear images with various conditions, i.e., stained cell colorations, background illumination, cytoplasm granule conditions, maturation stage and altered morphology. (a) Eosinophil cell granules clearly recognize in high quality image. (b) Granules are hard to identify in low quality image. (c) Normal round shape of a lymphocyte cell. (d) A deformed lymphocyte shape cell with an altered cell shape. (e,f) Lymphocytes and (g,h) neutrophils at different cell maturation stages.

Furthermore, some observations are based on nucleus morphology, for example, lobed versus round, polymorphonuclear or mononuclear shape, cell size, and the presence of cell cytoplasm granules, are common characteristics used for characterization of WBCs [20]. After the features are extracted, machine learning and neural networks (NN) are widely used for cell classification.

Unique features such as morphology, nucleus shape, and presence of cytoplasm granules significantly help the expert-system to classify the cells, including detecting abnormal cells. However, all interpretations from the blood smear images are highly dependent on the quality of the blood smear preparation. The quality varies between labs [21] and the instruments used to acquire the images since they have various microscopes and camera systems [22-23]. Thus, the staining processes and imaging instruments also produce variations of nucleus coloration, cytoplasm, and background that may result in image distortions. For example, the cytoplasm granules can be used as a texture feature that provides unique identification of a cell. Unfortunately, these granules are very small. Sometimes the textures are almost invisible due to the quality of staining, poor lighting, and image resolution. These decrease the quality of the sample image. Hence, information about granule presence is typically inconsistent and very difficult to use as a significant cell feature for classification. Therefore, geometric features, such as shape, are useful features for differentiating WBC types [24-25].

In this work, we utilized the HOG as a feature defining WBC nuclei and applied a simple technique for WBC segmentation from blood smear images. To the best of our knowledge, HOG feature are typically used in object detection, e.g., human recognition, and are useful in object shape pattern recognition. Nevertheless, implementation of this feature yet to be performed specifically in WBC classification of blood smear images. The information on edge or gradient features is very characteristic of local shape. Thus, we expected that object classification, such as for cell nuclei, could be achieved using this feature. Therefore, in our work, we applied HOG to determine shape features of cell nuclei. Furthermore, the HOG feature might be useful for other applications of interest concerning the shapes of nuclei or cells. Additionally, others feature algorithms could be associated with HOG feature. Figure 1 shows an example of microscopic peripheral blood smear images. The images show examples of cells coloration, variation of background illumination, cytoplasm granules and cell nucleus conditions including cell maturation stages and deformed cells with completely altered morphology and image quality.

3. Materials and methods

We proposed simple color thresholding and K-means clustering for WBC segmentation based on YCbCr Luminance (Y), with chrominance information for blue and red component (Cb and Cr) color spaces. These segmentation steps are essential as the accuracy of the feature extraction and classification depends on correct segmentation of cell nuclei. Therefore, our proposed method overcomes the problems associated with low-quality blood smear images, e.g., non-uniform background lighting, dye colorations, inconsistency cytoplasm, and granule information, among others. Color thresholding was used to eliminate most of the red blood cells (RBCs) and artifacts. Artifacts are due to dust particles and clots of stain or dye residues in a blood smear image. However, a single thresholding process cannot remove all of the features, such as RBCs and artifacts. Therefore, further segmentation of WBC nuclei using K-means clustering separated the cell cytoplasm and nuclei. The cytoplasm usually has a pink color and the cell nucleus is blueish. Therefore, K-means clustering is more practical than conventional color thresholding. Segmented WBC nucleus image features are then extracted using HOG to classify various types of WBCs, basophils, eosinophils, lymphocytes, monocytes, and neutrophils using a Support Vector Machine (SVM) and artificial neural networks (ANN). Figure 2 shows the framework of WBC classification.

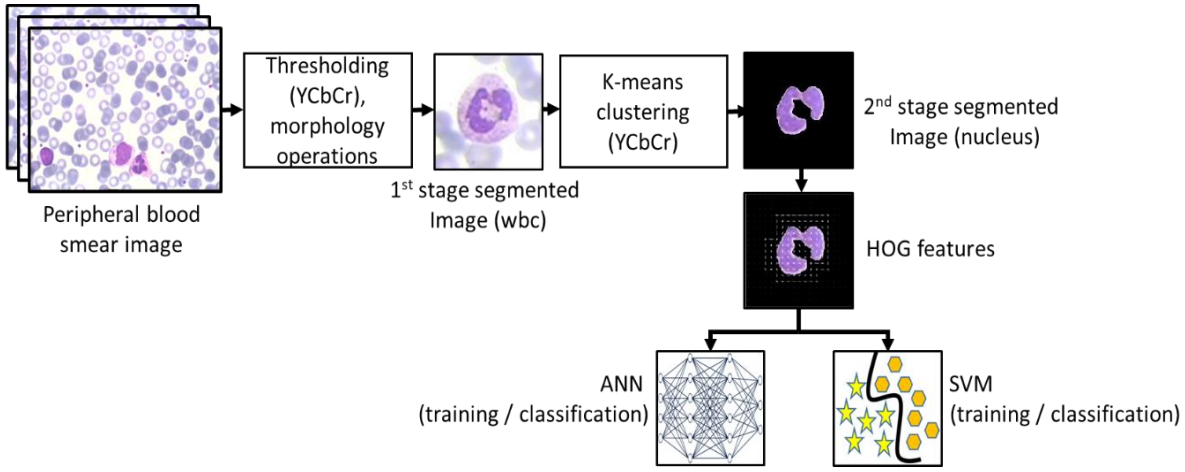

Figure 2 Framework of WBC classification using the HOG feature

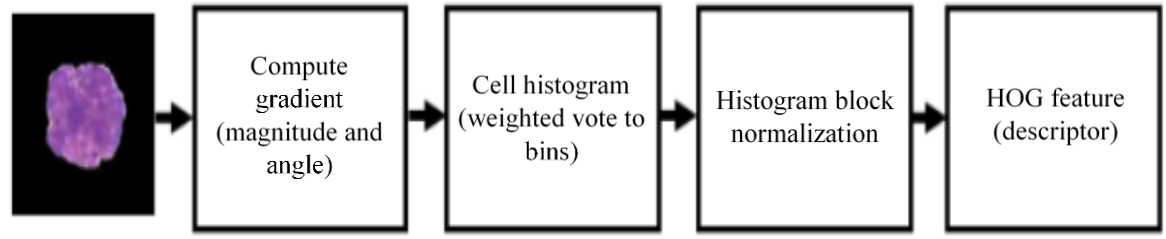

Figure 3 Block diagram of HOG feature extraction algorithm

3.1 Microscopic blood smear images

Microscopic blood smear images were derived from leukocyte images for a segmentation and classification (LISC) database [26]. Peripheral blood hematological images were taken from healthy subjects. The blood samples were smeared and stained using the Gismo-Right technique. Images were acquired using a light microscope (Axioskope 40, Carl Zeiss, Germany) at a magnification of 100X and captured using a digital camera (SSCDC50AP, Sony, Japan) at a resolution of 720×576 pixels. Images were captured and classified by a hematologist as normal WBCs, basophils, eosinophils, lymphocytes, monocytes, and neutrophils.

3.2 White blood cell and nucleus segmentation

Macroscopic blood smear images are segmented twice. In the first step, the segmentation is conducted using a color threshold method based on the YCbCr color space. The minimum threshold value that is suitable for these database images is 125 for Cb and 137 for Cr. A pre-processing step such as color adjustment or histogram equalization is not required. The database provides various image conditions such as the stained cell color and overall quality of images. Color thresholding eliminates most of the RBC objects in the image. Most of the RBC colors are pink to reddish or sometimes blueish, containing staining dye residues that have a similar color as stained WBCs. Therefore, color thresholding provides better performance in the segmented image. Next, we performed morphology filtering to clean the remaining artifacts in the image and segment the WBC to a size of 150x150 pixels, as shown in Figure 2. The selected image size was carefully determined for all types of WBCs to be used later for HOG feature extraction. The reason for choosing this size was to maintain the original image size, where some of the WBCs, e.g., monocytes, are bigger than others cell types. Thus, resizing the segmented image is not recommended when changing the size of some of WBCs. This can increase the chance of cell misclassification.

K-means color clustering is used for segmenting a cell nucleus from the segmented WBC image in the second stage of the process. Then, we performed linear filtering for image enhancement, which reduced image noise and improved coloration effects. The image is segmented by clustering into five-color clusters in the YCbCr color space. The selection of color space was determined in our initial work. YCbCr demonstrated an appropriate segmentation of cell nuclei compared to other color spaces suitable for this database. Next, the maximum Cb and Cr color values are determined from the clustered objects, where nuclei with purplish to blueish colors are darker, with much lower color values than nuclei. To further enhanced the segmented nucleus image, morphology operations were used to remove remaining artifacts such as dye particles and filling small holes in the segmented nucleus image caused by image discoloration. Figure 2 shows the segmentation process.

3.3 Feature extraction

HOG has become very popular in the field of computer vision. The advantages of HOG are its capability to describe object-orientation while showing invariance to geometric and photometric transformations operating in localized regions. Furthermore, it is unaffected by changes in shapes and illumination in larger spatial regions. HOG can be implemented on both color or grayscale images, however,

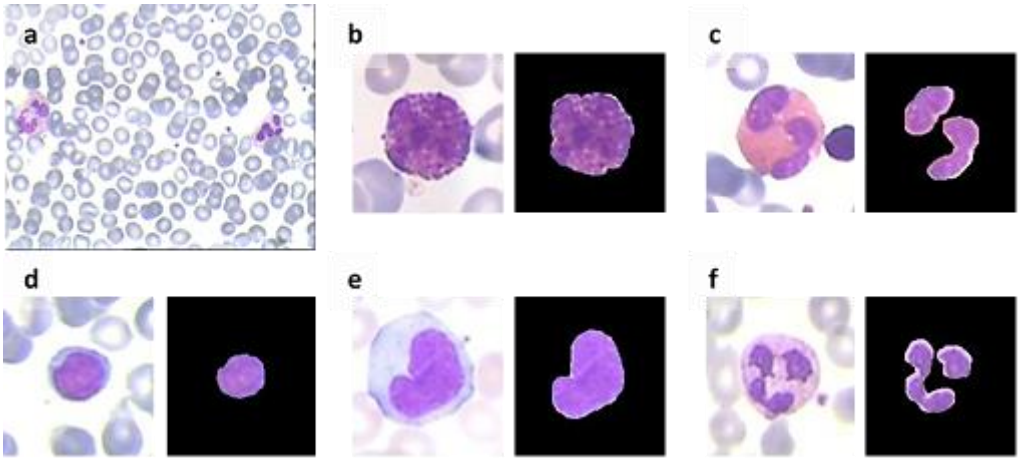

Figure 4 (a) A raw peripheral blood smear image from the dataset. (b-f) Segmented basophils, eosinophils, lymphocytes, monocytes and neutrophils, respectively, with a size of 150x150 pixels using a YCbCr color threshold and segmentation of cell nuclei using a K-means cluster technique

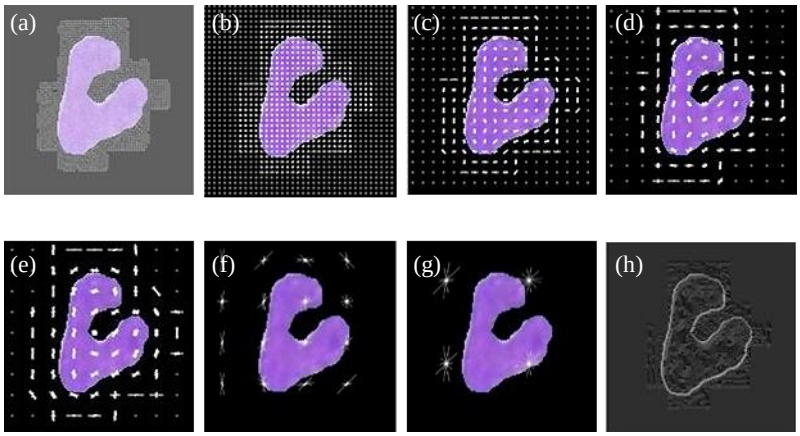

Figure 5 The HOG cell size parameter shows the effect of the amount of shape information encoded in a feature, (a-g) a monocyte nucleus image visualization of spatial information of HOG features of 2x2, 4x4, 8x8, 12x12, 16x16, 32x32, and 64x64 pixels, respectively, and (h) calculated magnitude and directional gradients of a nucleus image

color images yield slightly better performance [27-28]. The HOG components, such as the size of the HOG cell, i.e., cell size, are essential to provide details of an object's shape. However, a smaller cell size significantly increases the dimensionality of the HOG feature vector, which requires additional processing time. We evaluated the most efficient conditions suitable for nucleus cell classification by changing the HOG cell size. This helped to identify which cell size setting encodes enough spatial information to visually identify the shape of WBC nuclei while reducing the number of dimensions. Additionally, it helps to speed up the training and classification processes.

Another critical component in the HOG feature is the number of cells per block, i.e., the block size. The block size is the number of cells grouped together in larger blocks. Reducing the block size captures the gradient of local pixels. For example, a 2x2 cells block size is suitable for suppressing image illumination changes. The impact on the distribution in the histogram by changing the number of histogram bins on the classification performance will be evaluated because increasing the number of bins will reduce the orientation of the gradient range that each bin covers. Figure 3 shows the WBC nuclei feature extraction algorithm using the HOG feature.

3.4 WBC classification

A support vector machine (SVM) and artificial neural network (ANN) were used as classifiers. The performance of these methods is measured by determined the accuracy of the WBC class. The performance accuracy of a test is its capability to correctly differentiate the WBC classes, i.e., basophils, eosinophils, lymphocytes, monocytes, and neutrophils. Performance evaluation is conducted using four crucial parameters, True Positive (TP), True Negative (TN), False Positive (FP) and False Negative (FN). TP is a WBC cell class observation that is positive and predicted to be positive. TN is a WBC cell class observation that is negative and predicted to be negative. FP is a WBC cell class observation that is negative but predicted positive. Finally, FN is a WBC cell class observation that is positive but is predicted negative by the system. The performance accuracy is calculated as:

$$\text{Accuracy} = \frac{TP+TN}{TP+FP+FN+TN}$$

4. Results

4.1 WBC nucleus segmentation

Table 1 The accuracy of WBC nucleus classification using a SVM and varying the HOG cell size and histogram bins

Cell size	Bins	Classification Accuracy (%)					Avg. acc. (%)
		Basophil	Eosinophil	Lymphocyte	Monocyte	Neutrophil	
2X2	10	76.3	75.4	74.5	81.2	71.3	75.7
2X2	15	83.2	74.4	75.7	76.7	72.8	76.6
2X2	20	79.2	74.6	88.1	75.5	75.3	78.5
2X2	25	88.2	71.5	82.3	86.7	67.8	79.3
4x4	10	85.4	82.3	75.7	88.3	75.5	81.4
4x4	15	83.8	77.4	80.6	88.6	74.8	81.0
4x4	20	86.3	83.4	81.2	92.8	80.6	84.9
4x4	25	89.1	79.1	85.4	83.7	75.9	82.6
8x8	10	87.4	67.8	92.7	84.6	87.7	84.0
8x8	15	90.6	69.4	91.7	84.8	88.1	84.9
8x8	20	92.1	69.8	92.3	87.4	86.7	85.7
8x8	25	85.7	70.2	91.4	81.4	86.2	83.0
12x12	10	91.2	71.9	89.5	83.2	90.5	85.3
12x12	15	89.7	73.3	91.6	87.4	91.4	86.7
12x12	20	90.1	75.4	88.4	83.7	91.7	85.9
12x12	25	86.9	72.3	91.2	86.6	89.9	85.4
16x16	10	89.7	68.9	91.4	83.4	88.3	84.3
16x16	15	91.1	73.7	92.5	86.1	88.2	86.3
16x16	20	92.3	74.6	92.7	87.2	91.1	87.6
16x16	25	91.4	74.3	93.7	84.6	88.8	86.6
32x32	10	90.4	75.5	86.5	100	87.9	88.1
32x32	15	94.3	77.4	94.3	94.5	86.5	89.4
32x32	20	94.3	75.7	91.2	97.8	88.4	89.5
32x32	25	94.1	69.5	91.7	97.6	85.7	87.7
64x64	10	70.5	60.3	72.3	69.4	52.4	65.0
64x64	15	70.3	50.5	76.5	67.3	54.3	63.8
64x64	20	71.1	48.1	76.7	71.4	55.1	64.5
64x64	25	75.2	48.1	75.8	76.2	55.3	66.1

Table 2 The accuracy of WBC nucleus classification using a SVM based on histogram bin average for each HOG cell size

Cell size (pixels)	Average classification Accuracy (%)					Average accuracy (%)
	Basophil	Eosinophil	Lymphocyte	Monocyte	Neutrophil	
2x2	81.7	74.0	80.2	80.0	71.8	77.5
4x4	86.2	80.6	80.7	88.4	76.7	82.5
8x8	89.0	69.3	92.0	84.6	87.2	84.4
12x12	89.5	73.2	90.2	85.2	90.9	85.8
16x16	91.1	72.9	92.6	85.3	89.1	86.2
32x32	93.3	74.5	90.9	97.5	87.1	88.7
64x64	71.8	51.8	75.3	71.1	54.3	64.8

The segmented cell nucleus from a two-step segmentation process based on YCbCr color thresholding and K-means clustering techniques with a minimum value color threshold, using a minimum value of 125 for Cb and 137 for Cr are appropriate for all dataset images of all five types of WBCs i.e., basophils, eosinophils, lymphocytes, monocytes, and neutrophils. The 150x150 pixels segmented images are suitable for all datasets. Figure 4 shows an example of a raw microscopic blood smear image and segmented WBC with its cell nucleus.

4.2 HOG feature extraction

The HOG feature vectors were calculated from the segmented nucleus cells of the training images by varying the cell size and number of bins. Increasing the cell size reduces the image detail and increases the number of bins. This will increased the size of the feature vector, which requires more time to extract the features. Selection of the correct degree of HOG feature vector in needed to encode the object information correctly. In this work, HOG cell sizes were varied as 2x2, 4x4, 8x8, 16x16, 32x32 and 64x64 pixels. In terms of histogram bins, the variation were 10, 15, 20 and 25 for each cell size. Figure 5 shows an example of HOG feature visualization on a nucleus of each cell size. A cell size of 2x2 pixels encodes highly detailed nucleus shape information but increases the HOG feature vector dimensions. However, a cell size of 64x64 reduced shape information with significantly lower feature vector dimensionality.

4.3 Performance of WBC classification using SVM

Supervised learning with SVM based classifiers using a quadratic kernel function was employed to map the training data into kernel space. A Sequential Minimal Optimization (SMO) method was used to find the separating hyperplane and a one-to-one architecture was used for classification. The total images of each of five types of WBC considered 180 cells, i.e., a total of 900 images. To reduce training data overfitting, five-fold cross-validation was used. Table 1 shows the results of classification accuracy by varying the HOG cell size and histogram bin parameters using a SVM classifier. Table 2 shows the histogram bins overall average accuracy for each type of WBC.

Table 3 The accuracy of WBC nucleus classification using a SVM varying the HOG cell size and histogram bins using ANN

Cell size	Bins	Classification accuracy (%)					Avg. acc. (%)
		Basophil	Eosinophil	Lymphocyte	Monocyte	Neutrophil	
2X2	10	93.0	96.3	98.9	95.4	87.4	94.2
2X2	15	95.0	96.2	95.8	93.5	94.4	95.0
2X2	20	94.0	96.0	95.2	96.0	94.5	95.1
2X2	25	97.6	92.9	97.7	88.8	96.6	94.7
4x4	10	93.2	94.5	95.6	90.7	97.2	94.2
4x4	15	94.9	92.1	96.7	93.5	98.2	95.1
4x4	20	95.5	94.2	95.7	96.1	93.4	95.0
4x4	25	96.2	93.4	97.8	95.1	95.5	95.6
8x8	10	94.1	96.0	94.6	96.0	97.2	95.6
8x8	15	96.7	95.5	97.8	97.7	96.7	96.9
8x8	20	100.0	95.0	96.7	99.4	96.7	97.6
8x8	25	96.2	98.3	95.6	98.3	93.2	96.3
12x12	10	98.9	95.6	98.3	98.3	96.7	97.6
12x12	15	98.9	95.0	98.9	97.8	95.1	97.1
12x12	20	97.3	95.0	98.9	97.7	95.6	96.9
12x12	25	97.3	96.2	97.2	97.7	96.7	97.0
16x16	10	98.3	96.4	98.9	96.1	95.6	97.1
16x16	15	98.9	97.1	98.3	95.0	96.2	97.1
16x16	20	98.4	97.7	100.0	98.3	94.7	97.8
16x16	25	100.0	95.0	97.3	95.1	95.6	96.6
32x32	10	98.9	92.4	98.9	97.7	96.0	96.8
32x32	15	96.8	88.6	98.9	94.9	89.8	93.8
32x32	20	97.2	89.4	96.2	97.0	90.9	94.1
32x32	25	96.2	90.6	97.2	97.1	90.9	94.4
64x64	10	92.3	81.2	86.9	81.6	75.5	83.5
64x64	15	93.5	80.1	92.0	84.6	81.3	86.3
64x64	20	94.0	76.5	88.9	80.4	79.4	83.8
64x64	25	93.0	77.2	88.2	84.7	79.6	84.5

Table 4 The accuracy of WBC nucleus classification using ANN based on histogram bin averages for each HOG cell size

Cell size	Average classification accuracy (%)					Average accuracy (%)
	Basophil	Eosinophil	Lymphocyte	Monocyte	Neutrophil	
2x2	94.9	95.4	96.9	93.4	93.2	94.8
4x4	95.0	93.6	96.5	93.9	96.1	95.0
8x8	96.8	96.2	96.2	97.9	96.0	96.6
12x12	98.1	95.5	98.3	97.9	96.0	97.2
16x16	98.9	95.8	98.6	96.1	95.5	97.0
32x32	97.3	90.3	97.8	96.7	91.9	94.8
64x64	93.2	78.8	89.0	82.8	79.0	84.5

4.4 Performance of WBC classification using ANN

900 images of each of five types of WBC were divided randomly so that 60% were used for network training, 20% for network validation and 20% for network generalization. The model used is a two-layer feedforward network, scaled conjugate gradient backpropagation training method with a sigmoid transfer function in 10 hidden layers, and a softmax output layer. We trained the network multiple times to get the highest overall classification accuracy and a satisfactory mean square error (MSE). Table 3 shows the results of classification accuracy when varying the HOG cell size and histogram bin parameters using ANN. Table 4 shows the histogram bin overall average accuracy for each type of WBC.

5. Discussion

The overall average accuracy shows that the ANN model is the most efficient and outperforms the support vector machine, as shown in Tables 1 and 3, with more than a 10% accuracy discrepancy. The reason for the success of the ANN model is its ability to minimize error in the iterative procedure of optimizing its parameters, such as the learning rate. Alternatively, the SVM method has a predefined value of some input parameters that are hard to define. Furthermore, the HOG feature descriptor is very large depending on the HOG input parameters, such as cell size, number of bins, and overlapping cells, among others, which sometimes require higher dimension of data. Thus, the ANN demonstrated its ability to handle these high dimensional features effectively.

The performance accuracy shows marginal differences when the cell size is increased for both classifiers. The accuracy drops significantly at a larger cell size of 64x64 pixels for both the SVM and ANN classifiers. This is because the dimensions of the feature vectors reduce the information about the object shape, as visualized in Figure 5. Therefore, a high number of cells for small object detection it is not suitable for implementation. Hence, the appropriate HOG cell size value for a 150x150 pixels image of a WBC nucleus shows that cell sizes of 8x8, 12x12 and 16x16 pixels provides better performance than the other sizes using an ANN classifier, as shown in Table 3. The SVM classifier also

yielded similar results to ANN. However, the performance is different when with a cell size of 32x32 pixels. The 32x32 pixels cell size yields the highest performance, as shown in Table 2. Alternatively, ANN performance begins to drop when the cell size increases, compared to a SVM, as shown in Table 4, where the highest performance was with a cell having 32x32 pixels. This suggests that increasing feature descriptors provides excellent performance for the ANN model but not for the SVM.

For both classifiers, the number of histogram bins has an insignificant influence on the overall performance. The reason is that the HOG algorithm, as shown in Figure 3, uses a histogram block normalized to all feature vectors. Therefore, a fewer number of bins does not provide enough spatial information about the oriented gradient and would increase the detection error tradeoff, i.e., miss rate performance. A greater number of bins, e.g., 9, makes only a little difference in classification performance [29].

A smaller cell number provides better details of object spatial information, as shown in Figure 5. However, from the results, we noticed that for a smaller HOG cell size, less than 8x8 pixels, the results of classification performance decreased significantly for both SVM and ANN classifiers. The feature descriptor, for example, using a cell size of 2x2 pixels on a 150x150 pixels input image introduced a few hundreds of thousands of dimensions, i.e., high-dimensional spaces. The high dimensions of the feature data resulted in the disadvantage of dimensionality and increased computational costs. Furthermore, when the feature dimensionality increases, the volume of the space increases so fast that the available data becomes sparse and results in low performance. Increasing the datasets, such as training data or reducing the features, could avoid the sparse data problem [30].

6. Conclusions

We performed classification of WBC nucleus type based on the HOG feature. The results show that the HOG feature is suitable for cell-shape classification applications with high accuracy. Further cell optimization, such as reducing the feature dimensionality or selection of most discriminative features, is recommended. HOG combined with other cell features such as texture and color, among others are suggested to develop a robust system with increased performance. This HOG feature is suitable for implementation in other cell analysis applications.

7. References

[1] Pierre RV. Peripheral blood film review: the demise of the eyecount leukocyte differential. Clin Lab Med. 2002;22(1):279-97.

[2] Nazlibilek S, Karacor D, Ercan T, Sazli MH, Kalender O, Ege Y. Automatic segmentation, counting, size determination and classification of white blood cells. Meas J Int Meas Confed. 2014;55:58-65.

[3] Ghosh P, Bhattacharjee D, Nasipuri M. Blood smear analyzer for white blood cell counting: a hybrid microscopic image analyzing technique. Appl Soft Comput J. 2016;46:629-38.

[4] Di Ruberto C, Loddo A, Putzu L. A leucocytes count system from blood smear images: segmentation and counting of white blood cells based on learning by sampling. Mach Vis Appl. 2016;27(8):1151-60.

[5] Ravikumar S. Image segmentation and classification of white blood cells with the extreme learning machine and the fast relevance vector machine. Artif Cells Nanomedicine Biotechnol. 2016;44(3):985-9.

[6] Sajjad M, Khan S, Jan Z, Muhammad K, Moon H, Kwak JT, et al. Leukocytes classification and segmentation in microscopic blood smear: a resource-aware healthcare service in smart cities. IEEE Access. 2017;5:3475-89.

[7] Sarrafzadeh O, Rabbani H, Talebi A, Banaem HU. Selection of the best features for leukocytes classification in blood smear microscopic images. In: Gurcan MN, Madabhushi A, editors. Medical Imaging 2014: Digital Pathology; 2014 Feb 16-17; California, United States. USA: SPIE; 2014. p. 90410P.

[8] Saraswat M, Arya KV. Automated microscopic image analysis for leukocytes identification: a survey. Micron. 2014;65:20-33.

[9] Hiremath PS, Bannigidad P, Geeta S. Automated identification and classification of white blood cells (Leukocytes) in digital microscopic images. IJCA Special Issue on Recent Trends Image Process and Pattern Recognition. 2010:59-63.

[10] Shirazi SH, Umar AI, Naz S, Razzak MI. Efficient leukocyte segmentation and recognition in peripheral blood image. Technol Heal Care. 2016;24(3):335-47.

[11] Sabino DMU, Da Fontoura Costa L, Rizzatti EG, Zago MA. A texture approach to leukocyte recognition. Real-Time Imaging. 2004;10(4):205-16.

[12] Li X, Cao Y. A robust automatic leukocyte recognition method based on island-clustering texture. J Innov Opt. Health Sci. 2015;9(1):1650009.

[13] Sarrafzadeh O, Dehnavi AM, Banaem HY, Talebi A, Gharibi A. The best texture features for leukocytes recognition. J Med Signals Sens. 2017;7(4):220-7.

[14] Hegde RB, Prasad K, Hebbar H, Singh BMK. Development of a robust algorithm for detection of nuclei of white blood cells in peripheral blood smear images. Multimed Tool Appl. 2019;78:17879-98.

[15] Zhang C, Xiao X, Li X, Chen YJ, Zhen W, Chang J, et al. White blood cell segmentation by color-space-based k-means clustering. Sensors. 2014;14(9):16128-47.

[16] Nazlibilek S, Karacor D, Ertürk KL, Sengul G, Ercan T, Aliew F. White blood cells classifications by SURF image matching, PCA and dendrogram. Biomed Res. 2015;26(4):633-40.

[17] Al-Dulaimi K, Chandran V, Banks J, Tomeo-Reyes I, Nguyen K. Classification of white blood cells using bispectral invariant features of nuclei shape. 2018 Digital Image Computing: Techniques and Applications (DICTA); 2018 Dec 10-13; Canberra, Australia. USA: IEEE; 2018. p. 1-8.

[18] Benazzouz M, Baghli I, Chikh MA. Microscopic image segmentation based on pixel classification and dimensionality reduction. Int J Imaging Syst Technol. 2013;23(1):22-8.

[19] Nikitaev VG, Nagornov OV, Pronichev AN, Polyakov EV, Dmitrieva VV. The use of the wavelet transform for the formation of the quantitative characteristics of the blood cells images for the automation of hematological diagnostics. WSEAS Trans Biol Biomed. 2015;12:16-9.

[20] Prinyakupt J, Pluempitiwiriyawej C. Segmentation of white blood cells and comparison of cell morphology by linear and naïve Bayes classifiers. Biomed Eng Online. 2015;14(1):1-19.

[21] Adewoyin AS, Nwogoh B. Peripheral blood film - a review. Ann Ib Postgrad Med. 2014;12(2):71-9.
[22] Riley RS, Ben-Ezra JM, Massey D, Cousar J. The virtual blood film. Clin Lab Med. 2002;22(1): 317-45.
[23] Yu H, Ok CY, Hesse A, Nordell P, Connor D, Sjostedt E, et al. Evaluation of an automated digital imaging system, nextslide digital review network, for examination of peripheral blood smears. Arch Pathol Lab Med. 2012;136(6):660-7.
[24] Ghosh M, Das D, Mandal S, Chakraborty C, Pala M, Maity AK, et al. Statistical pattern analysis of white blood cell nuclei morphometry. 2010 IEEE Students Technology Symposium (TechSym); 2010 Apr 3-4; Kharagpur, India. USA: IEEE; 2010. p. 59-66.
[25] Gautam A, Bhadauria H. Classification of white blood cells based on morphological features. International Conference on Advances in Computing, Communications and Informatics (ICACCI); 2014 Sep 24-27; New Delhi, India. USA: IEEE; 2014. p. 2363-8.
[26] Rezatofighi SH, Soltanian-Zadeh H. Automatic recognition of five types of white blood cells in peripheral blood. Comput Med Imaging Graph. 2011;35(4):333-43.
[27] Ott P, Everingham M. Implicit color segmentation features for pedestrian and object detection. IEEE 12th International Conference on Computer Vision; 2009 Sep 29-Oct 2; Kyoto, Japan. USA: IEEE; 2009. p. 723-30.
[28] Creusen IM, Wijnhoven RGJ, Herbschleb E, De With PHN. Color exploitation in hog-based traffic sign detection. IEEE International Conference on Image Processing; 2010 Sep 26-29; Hong Kong, China. USA: IEEE; 2010. p. 2669-72.
[29] Dalal N, Triggs B. Histograms of oriented gradients for human detection. IEEE Computer Society Conference on Computer Vision and Pattern Recognition (CVPR'05); 2005 Jun 20-25; San Diego, USA. USA: IEEE; 2005. p. 886-93.
[30] Domingos P. A Few Useful Things to Know About Machine Learning. Commun ACM. 2012;55(10): 78-87.